Title: Metabolic rates of glucose in the brain networks of healthy adults vary as a function of age and levels of peripheral insulin resistance, and predict cognition

Authors: Deery, H.A.[1.2], Liang, E.[1.2], Di Paolo, R.[1,2], Voigt, K., Murray, G., Siddiqui, M.N., Moran, C.[4], Egan, G.F.[1,2,3] and Jamadar, S.D.[1,2,3*]

Affiliations:

1. Turner Institute for Brain and Mental Health, Monash University, Wellington Rd, Melbourne, 3800, Australia.

2. Monash Biomedical Imaging, Monash University, 770 Blackburn Rd, Melbourne, 3800, Australia.

3. Australian Research Council Centre of Excellence for Integrative Brain Function, Melbourne, 3800, Australia.

4. School of Public Health and Preventive Medicine, Monash University, 553 St Kilda Rd, Melbourne VIC 3004.

***Corresponding author address:** Monash Biomedical Imaging, Monash University, 770 Blackburn Rd, Melbourne, 3800, Australia. **e-mail address:** sharna.jamadar@monash.edu;

Running headline: Cerebral glucose metabolism, age and insulin

Abstract

Research suggests that cerebral metabolic rates of glucose (CMR_{GLC}) decline with age. However, only a small body of research has taken into account partial volume effects in PET imaging and age-related reductions in cortical thickness. Separate research suggests that levels of peripheral insulin resistance may be a biomarker for functional brain changes. Thirty-six younger (mean 27.8 years) and 43 older (mean 75.5) participants completed a blood and cognitive tests battery and a simultaneous 90-minute MR/PET scan. Cortical thickness and CMR_{GLC} were derived using the Schaefer 100 atlas, and major subcortical structures. Insulin resistance was measured with the Homeostatic Model Assessment of Insulin Resistance (HOMA-IR). Older adults had lower CMR_{GLC} than younger adults across most regions, an effect that was mediated in part but not in full by age-related lower cortical thickness. Age x HOMA-IR interaction analysis showed that a 10% increase in insulin resistance was associated with 2% to 8% lower CMR_{GLC} in younger adults across regions, with smaller reductions in older adults. Higher CMR_{GLC} in the ventral attention, control and default networks was associated with better executive function, attention and processing seed. These results suggest that the age-related cerebral metabolism reductions are partly mediated by cortical atrophy, whereas insulin resistance associations with CMR_{GLC} are moderated by age.

Key words: Brain, metabolism, ageing, insulin, cognition.

1. Introduction

1.1 Glucose: Fuel for the Brain

Glucose is the primary source of energy for the brain, powering an array of functions including the generation of action and postsynaptic potentials and the synthesis of neurotransmitters.[1] Because of the brain's high demand for energy, a continuous supply of glucose is necessary to maintain brain health. Among healthy adults, the cerebral metabolic rate of glucose (CMR_{GLC}) has been reported in most regions to be in the order of 4-7 mg of glucose per 100ml per minute.[2] The rate of cerebral glucose metabolism is also considered to be a reliable measure of neuronal activity[1] and be related to cognitive performance in health[3] and disease.[4]

Cerebral metabolism is most commonly measured *in vivo* with F-18 fluorodeoxyglucose (18F-FDG or FDG) Positron Emission Tomography (PET). FDG is a glucose analogue that is trapped in neurons or glial cells after being metabolised into glucose-6-phosphate. The local concentrations of the tracer radioactivity can be measured using FDG-PET. The analysis of FDG kinetics and calculation of CMR_{GLC} is usually based on a compartment model originally developed by Sokoloff et al.[5] and refined by others.[6] The model uses the transport and clearance rates of the measured FDG tracer between the plasma and the tissue compartments, and the phosphorylation and dephosphorylation rate of the tracer. Kinetic models of FDG are used to convert the radioactivity compartment measurements to metabolic rates. For example, the Patlak graphical analysis technique[7] uses linear regression to analyse the kinetics of the tracer. With the inclusion of a term (the 'lumped constant') to adjust for the difference in uptake between normal glucose and FDG, as well as the plasma glucose level of the subject, CMR_{GLC} can be derived from the regression slope.[8]

In a recent systematic review and meta-analyses of FDG-PET studies in ageing, we found consistently lower CMR_{GLC} among older compared to younger adults.[2] Pooled effect size meta-analysis across 21 studies identified lowered CMR_{GLC} among older adults ranging from 8% in the occipital lobe to 12% in the frontal lobe. The association between lower CMR_{GLC} and older age was partially mediated by concurrent structural brain changes with ageing. In particular, the magnitude of the age-related reductions in CMR_{GLC} were lower but remained significant in the frontal and temporal regions after adjusting for grey matter atrophy. In the subcortical structures, the caudate showed lower CMR_{GLC} in older versus younger adults. An activation likelihood

estimates (ALE) meta-analysis of the concordance of neuroimaging results from eight PET studies showed nine clusters of lower CMR_{GLC} among older versus younger adults. The two largest and most concordant clusters were obtained in the left and right inferior frontal and superior temporal gyri and the insula. Taken together, these meta-analyses suggest that CMR_{GLC} differences in ageing are predominantly frontal and temporal and are mediated, at least in part, by brain atrophy.

Our systematic review and meta-analyses summarised the available research and identified several limitations in the existing literature. Many of the studies of CMR_{GLC} in ageing were conducted 20 or more years ago on scanners with relatively poor spatial resolution (see ref[2] and Table 1). Consequently, the *in vivo* quantification of CMR_{GLC} has mostly been limited to the whole brain or the lobular level. Whilst these studies have revealed large-scale CMR_{GLC} differences in ageing, they have limited ability to detect differences in smaller brain regions that relate to specific functional and cognitive processes. Furthermore, a relatively small number of PET studies adjusted for brain atrophy in ageing, imaging partial volume effects, or both.[9,10] Age-related declines in grey matter volume and thickness can reduce CMR_{GLC} calculated on a regional basis.[11] To better understand the role that brain atrophy plays in mediating the CMR_{GLC} and ageing relationship, adjustments must be made for cortical volume differences at the same spatial scale.

In the current study we address these limitations by investigating age differences in CMR_{GLC} after correction for partial volume errors and adjustment for cortical thickness differences at the same scale as the CMR_{GLC} measurement. The brain was parcellated into 100 cortical regions using the Schaefer atlas[12] and the major subcortical structures from the Automated Anatomical Labeling[13] atlas. The Schaefer 100 regions were categorised into seven networks and seventeen sub-networks, to assist interpretation of the regional results in the context of the large-scale functional organisation of the brain.

1.2 Insulin Resistance and Brain Function

Insulin is a peptide hormone secreted by the β-cells of the pancreas. In heathy people, insulin (together with glucagon, its primary counter-regulatory hormone), regulates blood glucose concentrations by facilitating cellular glucose uptake. Among its array of functions, insulin regulates carbohydrate, lipid and protein metabolism and promotes cell division and growth.[14,15]

Although the brain is not insulin-dependent in terms of glucose uptake via insulin-dependent transporters, the brain *uses* insulin for a range of functions, highlighted by the expression of insulin receptors in neurons and glia, the presence of circulating brain insulin, as well as localised insulin production.[16]

Insulin resistance describes how sensitive the body is to the effects of insulin. A person who is more insulin resistant (or has lower insulin sensitivity) requires larger amounts of insulin to lower blood glucose levels than a person who has less insulin resistance.[17] In clinical and research settings, insulin resistance is operationalised as the concentration-response relationship between plasma insulin and insulin-mediated whole body glucose disposal. The Homeostatic Model Assessment of Insulin Resistance (HOMA-IR) models the relationship between glucose and insulin dynamics. The model assumes a feedback loop between the liver and pancreatic β-cells in which glucose concentrations are regulated by insulin mediated hepatic glucose production, and insulin concentrations are regulated by the response of the β-cells to glucose concentrations. HOMA-IR has broad clinical and research application due its validity across a range of levels of insulin resistance and β-cell function.[18]

There are substantial individual differences in insulin resistance that may impact cerebral metabolism, including in individuals with no metabolic dysfunction. Metabolically healthy adults can have fasting insulin levels ranging from less than 5 to over 30 μU/ml.[19] In insulin resistant individuals, tissues in the periphery and the brain lose the ability to respond to normal insulin levels. The underlying mechanism driving insulin resistance have been well described (see ref[17] for a review). Insulin resistance is considered a hallmark characteristic of Type 2 diabests[18] other cardiometabolic diseases and dementia, such as metabolic syndrome, heart disease and Alzheimer's disease.[20,21] As a result, most of the neuroimaging research on insulin-related brain changes has been in populations with a diagnosis of insulin resistance (see ref[22] for a review).

Some research has also investigated the relationship between HOMA-IR and CMR_{GLC} in older adults free of a diagnosis of insulin resistance, although the results have been inconsistent. In samples with an average age in the 60s and 70s, HOMA-IR has shown both a negative association[24] and no significant association[25] with whole-brain FDG uptake. Whole brain CMR_{GLC} was found to be lower in a sample of middle age adults comprising individuals both meeting or on average approaching a HOMA-IR threshold for insulin resistance.[23] A higher HOMA-IR has

been associated with lower glucose uptake in the thalamus and in the caudate of older adults without a diagnosis of insulin resistence[26], as well as in regions of the prefrontal, cingulate, temporal, insula, and posteromedial cortices.[24]

To our knowledge, research has not investigated the relationship between HOMA-IR and CMR_{GLC} in younger adults free of a diagnosis of insulin resistance, despite the fact that insulin levels can vary widely in non-clinical populations, and a loss of insulin sensitivity and changes in glycemia typically begin to occur years before a clinical diagnosis of insulin resistance.[27] In the current study, we investigate the relationship between CMR_{GLC} and HOMA-IR in younger and older adults free of a diagnosis of insulin resistance and diabetes. We also assess the relationship between CMR_{GLC} and cognition, and the possible moderating role of insulin resistance.

In this pre-registered report, we first hypothesised that greater cortical thickness would be associated with higher CMR_{GLC}. Our second hypothesis was that older adults would have lower cortical thickness and lower CMR_{GLC} than younger adults, and that cortical thickness would mediate some of the age differences in CMR_{GLC}. Our third hypothesis was that older adults would have greater HOMA-IR than younger adults, and that the association between HOMA-IR and CMR_{GLC} would be moderated by age, with the effect being stronger in older adults. Our final hypothesis was that greater CMR_{GLC} would be associated with better cognitive test performance.

2. Method

The study protocol was reviewed and approved by the Monash University Human Research Ethics Committee in accordance with Australian Code for the Responsible Conduct of Research (2007) and the Australian National Statement on Ethical Conduct in Human Research (2007). Administration of ionizing radiation was approved by the Monash Health Principal Medical Physicist, following the Australian Radiation Protection and Nuclear Safety Agency Code of Practice (2005). For participants older than 18 years, the annual radiation exposure limit of 5 mSv applies. The effective dose in this study was 4.9 mSv.

This study design, hypotheses and analyses were preregistered at OSF registrations (https://osf.io/93mnd).

2.1 Participants

Ninety participants were recruited from the general community via local advertising. An initial screening interview ensured that participants had the capacity to provide informed consent, did not have a history of hypertension, a diagnosis of diabetes, neurological or psychiatric illness, and were not taking psychoactive medication that could affect cognitive function or metabolism. Participants were also screened for claustrophobia, non-MR compatible implants, and clinical or research PET scan in the past 12 months. Women were screened for current or suspected pregnancy. Participants received a $100 voucher for participating in the study.

Eleven participants were excluded from further analyses due to blood haemolysis or well counter issues preventing insulin measurement or kinetic modelling (n=7), excessive head motion (n=2) or incomplete PET scan or image reconstruction (n=2).

2.2 Demographic Variables and Neuropsychological Test Battery

Prior to the scan, participants completed an online demographic and lifestyle questionnaire including age, sex, education, height and weight, history of smoking, alcohol and recreational drug use. Participants also completed a cognitive test battery consisting of measures of general intelligence, working memory, cognitive flexibility, inhibitory control and verbal learning (see Supplemental Information).

2.3 Simultaneous MR-PET Data Acquisitions

Participants underwent a 90-minute simultaneous MR-PET scan in a Siemens (Erlangen) Biograph 3-Tesla molecular MR scanner. Participants were directed to consume a high-protein/low-sugar diet for the 24 hours prior to the scan. They were also instructed to fast for six hours and to drink 2–6 glasses of water. Prior to FDG infusion, participants were cannulated in the vein in each forearm and a 10ml baseline blood sample taken. At the beginning of the scan, half of the 260 MBq FDG tracer was administered via the left forearm as a bolus, providing a strong PET signal from the beginning of the scan. The remaining 130 MBq of the FDG tracer dose was infused at a rate of 36ml/hour over 50 minutes, minimising the amount of signal decay over the course of the data acquisition. We have previously demonstrated that this protocol provides a good balance between a fast increase in signal-to-noise ratio at the start of the scan, and maintenance of signal-to-noise ratio over the duration of the scan.[28]

Participants were positioned supine in the scanner bore with their head in a 32-channel radiofrequency head coil and were instructed to lie as still as possible. The scan sequence was as follows. Non-functional MRI scans were acquired during the first 12 minutes, including a T1 3DMPRAGE (TA = 3.49 min, TR = 1640ms, TE = 234ms, flip angle = 8°, field of view = 256 × 256 mm^2, voxel size = 1.0 × 1.0 × 1.0 mm^3, 176 slices, sagittal acquisition) and T2 FLAIR (TA = 5.52 min, TR = 5,000ms, TE = 396ms, field of view = 250 × 250 mm^2, voxel size = .5 × .5 × 1 mm^3, 160 slices) to image the anatomical grey and white matter structures, respectively. Thirteen minutes into the scan, list-mode PET (voxel size = 2.3 x 2.3 x 5.0mm^3) and T2* EPI BOLD-fMRI (TA = 40 minutes; TR = 1000ms, TE = 39ms, FOV = 210 mm^2, 2.4 × 2.4 × 2.4 mm^3 voxels, 64 slices, ascending axial acquisition) sequences were initiated. A 40-minute resting-state scan was undertaken in naturalistic viewing conditions watching a movie of a drone flying over the Hawaii Islands. At 53 minutes, pseudo-continuous arterial spin labelling (pc-ASL) began, and at 58 minutes, diffusion-weighted imaging (DWI) was acquired with 71 directions to index white matter connectivity. pcASL, DWI and fMRI results are not reported here.

Plasma radioactivity levels were measured throughout the duration of the scan. Beginning at 10-minutes post infusion onset, 5ml blood samples were taken from the right forearm using a vacutainer at 10-minute intervals for a total of nine samples. The blood sample were immediately placed in a Heraeus Megafuge 16 centrifuge (ThermoFisher Scientific, Osterode, Germany) and spun at 2,000 rpm (RCF ~ 515g) for 5 minutes. 1,000-μL plasma was pipetted, transferred to a counting tube, and placed in a well counter for four minutes. The count start time, total number of counts, and counts per minute were recorded for each sample.

2.3.1 MRI Pre-Processing, Cortical Thickness and Grey matter Volume

For the structural T1 images, the brain was extracted in Freesurfer; quality of the pial/white matter surface was manually checked and corrected. Corrected Freesurfer surfaces were registered to MNI152 space using Advanced Normalization Tools (ANTs). Cortical thickness for the Schaefer 100 regions were obtained from the Freesurfer reconstruction statistics for each participant. Freesurfer calculates cortical thickness as the closest distance from the grey and white matter boundary to the grey matter and cerebrospinal fluid boundary at each vertex.[29,30] Although our primary analyses presented in the results section are focussed on cortical thickness, we also obtained grey matter volume from Freesurfer and report models including it in the supplementary

materials. Grey matter volume and cortical thickness have been shown be independent at the whole brain and regional level and genetically uncorrelated.[31] Grey matter volume is calculated from both surface area and cortical thickness as the amount of grey matter that lies between the grey-white interface and the pia mater.[31]

2.3.2 PET Image Reconstruction and Pre-Processing

The list-mode PET data for each subject were binned into 344 3D sinogram frames of 16s intervals. Attenuation was corrected via the pseudo-CT method for hybrid PET-MR scanners.[31] Ordinary Poisson-Ordered Subset Expectation Maximization algorithm (3 iterations, 21 subsets) with point spread function correction was used to reconstruct 3D volumes from the sinogram frames. The reconstructed DICOM slices were converted to NIFTI format with size 344 × 344 × 127 (voxel size: 2.09 × 2.09 × 2.03 mm3) for each volume. All 3D volumes were temporally concatenated to form a single 4D NIFTI volume. After concatenation, the PET volumes were motion corrected using FSL MCFLIRT[33], with the mean PET image used to mask the 4D data.

2.3.3 Correction for Partial Volume Effects

PET images were corrected for partial volume effects using the modified Müller-Gartner method implemented in PetSurf (https://surfer.nmr.mgh.harvard.edu/fswiki/PetSurfer).[34,35] The method corrects for white matter spill in and grey matter spill out of the PET signal. The equation subtracts from the grey matter voxel signal the white matter signal (convoluted by the point spread function) and divides by the grey matter signal. This division can introduce over-correction at the grey matter boundary, and hence a grey matter binary mask is recommended, with the threshold level needing to be chosen. A grey matter threshold of 20-30% is recommended in ageing because atrophy can influence results.[34] For our analyses, we chose a 25% grey matter threshold and surface-based spatial smoothing.[35] We used a Gaussian kernel with a full width at half maximum of 12 mm to increase the signal-to-noise ratio. Subcortical structures were partial volume corrected and spatially smoothed in volume space and merged with the cortical data.

2.3.4 Cerebral Metabolic Rates of Glucose

Calculation of CMR_{GLC} was undertaken in PMOD 4.4 (http://www.pmod.com) using the FDG time activity curves for the Schaefer 100 atlas parcellation and AAL subcortical structures. The FDG in the plasma samples was decay-corrected for the time between sampling and counting, and

used as the input function to the Patlak models. A lumped constant of 0.89[36] was used, and equilibrium (t) set at 10 mins, the time corresponding to the peak of the bolus and onset of a stable signal.[37] The fractional blood space (vB) was set at 0.05.[38] Participant's plasma glucose (mmol) was entered in the model from their baseline blood sample.

2.4 HOMA-IR

The baseline blood sample was used to collect 2ml of plasma for insulin and glucose measurement, which was undertaken by a commercial laboratory. HOMA-IR was calculated as fasting glucose (mmol/L) x fasting insulin (μU/ml) / 22.5.[39] The constant of 22.5 is a normalising factor for normal fasting plasma insulin and glucose (i.e., 4.5 mmol/L x 5 μU/ml = 22.5). Higher HOMA-IR values indicate greater insulin resistance.

2.5 Data Analysis

All analyses were run in SPSS version 29.0 (https://www.ibm.com/products/spss-statistics).

2.5.1. Demographics

For the demographic variables, independent sample t-tests for continuous variables and chi-square tests for categorical variables were undertaken and tested at uncorrected $p < 0.5$.

2.5.2. Association, Moderating and Mediating Effects of Age, HOMA-IR, Grey Matter Volume, Cortical Thickness and CMR_{GLC}

Hypothesis 1: To test hypothesis 1 – that there is a positive relationship between cortical thickness and CMR_{GLC} – Pearson correlations were calculated between cortical thickness and CMR_{GLC} in each Schaefer 100 region.

Hypothesis 2: To test hypothesis 2 - that after controlling for cortical thickness, there is a negative association between age group and insulin resistance (HOMA-IR) and CMR_{GLC} – point-biserial partial correlations of CMR_{GLC} and age group in the Schaefer 100 regions were calculated, controlling for cortical thickness in the same region. For the subcortical structures, whole brain average cortical thickness was used as a covariate.

We adopted the definition and analytic methods proposed by Baron and Kenny[40] to test for moderating and mediating variables (also see ref[41]). Specifically, cortical atrophy mediated the relationship between CMR_{GLC} and age when the following conditions were met: (1) there was a significant relationship between age and cortical thickness, (2) there was a significant association between age and CMR_{GLC}, and (3) when cortical thickness was controlled, the significant

relationship between age and CMR_{GLC} was reduced or no longer significant. Reduction in the association between age and CMR_{GLC} to zero was evidence that cortical thickness was the single, dominant mediator. When the association was reduced but non-zero, partial mediation was indicated (i.e., other factors were assumed to be involved). For each region, the size of the partial correlation was compared to the simple correlation of age group and CMR_{GLC}, and the difference in correlations was tested for significance using the procedure described by Raghunathan et al.[42] To test for a mediating effect of age on the relationship between insulin resistance and both cortical thickness and CMR_{GLC}, an age group x HOMA-IR product term was computed and used in the analyses with their main effects.[40] The models were tested for multicollinearity using the Variable Inflation Factor (VIF). If VIF was greater than 10, multicollinearity was considered to be an issue. In such cases, the highly correlated main effect was removed from the model. To illustrate and quantify the interaction, we calculated the slope of the regression line for younger and older adults in each region, and expressed the result as the % change in cortical thickness or CMR_{GLC} associated with a 10% change in HOMA-IR. Each series of correlations and partial correlations was FDR-corrected at $p < .05$ using the Benjamini and Hochberg method.[43]

Stepwise multiple regression analyses for CMR_{GLC} in each of the Schaefer 100 regions and the subcortical structures were undertaken to quantify the proportion of variance explained by the independent variables. For the age group and CMR_{GLC} relationship, cortical thickness was entered first, followed by the age group, and the change in r^2 was used to quantify how much variance age group explained beyond cortical thickness. For the HOMA-IR and CMR_{GLC} relationship, age group was entered first (cortical thickness was not included due to non-significant associations with CMR_{GLC}; see Table 4), followed by the HOMA-IR and the change in r^2 was calculated.

2.5.3. CMR_{GLC} and Cognition

Hypothesis 3: We applied data reduction techniques to reduce the dimensions in both the cognitive data and the number of brain regions. The cognitive scores were converted to Z-scores and entered in a Principal Component Analysis (PCA). Principal components (PCs) with eigenvalues greater than one were retained and subject to varimax rotation to optimally reduce dimensionality.[44] Participant component scores (regression weights) were saved for further analyses.

To reduce the dimensionality of glucose metabolism measures, CMR_{GLC} in each Schaefer 17 Network was calculated by volume-weighted averaging (using the PMOD regional volume) the Schaefer 100 regions within the 17 Networks. An overall subcortical CMR_{GLC} value was calculated using the volume-weighted CMR_{GLC} values from the subcortical structures. For cortical thickness, the Freesurfer area measure was used to derive an area-weighting factor for each of the Schaefer 100 regions within the corresponding 17 Network.

To test hypothesis 3 – that cognitive function negatively correlates with CMR_{GLC} after controlling for cortical thickness and age, and the relationships are moderated by the insulin resistance (HOMA-IR), a multivariate general linear model was used as follows. The five cognition PCs were entered as dependent variables, with CMR_{GLC} in 17 Networks entered as independent variables, together with age group and cortical thickness in the corresponding networks. If the multivariate model was significant for a specific network, post-hoc tests were then undertaken.

Where CMR_{GLC} in a Schaefer 17 Network was associated with cognition, a product term was calculated with HOMA-IR to test for a moderating effect. Separate multiple regression analyses were undertaken with the cognition principal component score as the dependent variable and the CMR_{GLC} x HOMA-IR product term entered as independent variable, together with age and cortical thickness. Because of high multicollinearity with the product term (VIF > 10), HOMA-IR was again excluded as a main effect.

3. Results

3.1 Demographic Factors

The final sample included 79 individuals, 36 younger (mean 27.8; SD 6.2; range 20-42 years) and 43 older (mean 75.5; SD 5.8; range 66-86 years) adults.

There was no significant difference in the proportion of females and males, years of education or body mass index between the older and younger adult groups (Table 1). However, older adults had lower whole brain grey matter volume, cortical thickness, systolic blood pressure (all $p < .001$) and resting heart rate ($p < .05$) compared to younger adults. Older adults also had higher fasting blood glucose levels, but no significant difference was found between groups for HOMA-IR. For younger adults, fasting blood glucose ranged from 4.0 to 5.4 mmol and HOMA-IR from 0.6 to 3.25. For older adults, fasting blood glucose ranged from 3.7 to 6.6 mmol and HOMA-IR from 0.1

to 3.14. The mean and standard deviation (SD) of CMR_{GLC} and cortical thickness for the younger and older adults are available in the supplementary materials (Table S1 and Figure S2).

Table 2 summarises the primary analyses related to Hypothesis 1 and 2, with detailed tables of results in the supplementary materials and discussed in the following sections..

3.2 Cortical Thickness and CMR_{GLC} (Hypothesis 1)

Higher CMR_{GLC} was associated with higher cortical thickness (see Figure 1, and Table S2) in 83 of the 100 regions, particularly in superior, middle and medial frontoparietal regions.

3.3 Age Association with Cortical Thickness and CMR_{GLC} (Hypothesis 2)

Older age was associated with lower cortical thickness in the Schaefer 100 regions, with the exception of some of the visual regions, the left temporal pole, and the right orbital frontal cortex (Table S2). Older age was also associated with lower CMR_{GLC} in the Schaefer 100 regions and subcortical structures, with the exception of some visual regions, both with and without controlling for cortical thickness (see Figure 2 and Table S2).

Lower r values were seen in all the Schaefer 100 regions and subcortical structures for the partial correlation between age group and CMR_{GLC} controlling for cortical thickness versus the correlation for age and CMR_{GLC} (see Table S2). The lower partial correlations indicate cortical thickness at least partially mediates the age and CMR_{GLC} relationship. In nine regions (8%), the reduction in the strength of the correlation after controlling for cortical thickness was statistically significant. However, the partial correlation remained above zero in all cases, suggesting the relationship is strongly but not fully mediated. For the remaining regions (92% of all regions), the correlation between age group and CMR_{GLC} was larger than the partial correlation controlling for cortical thickness, suggesting partial mediation of CMR_{GLC} by cortical thickness.

To quantify the degree that cortical thickness mediates the age and CMR_{GLC} relationship, the change in variance was examined in the blocks of the regression model (Tables 2 and S3). Cortical thickness explained between 0% and 34% of the variance in CMR_{GLC} in the Schaefer 100 regions and subcortical structures (block 1, cortical thickness and CMR_{GLC} relationship). Age explained 0% to 24% of additional variance in CMR_{GLC} over and above cortical thickness (block 2, effect of age on CMR_{GLC}).

The regions in which cortical thickness explained the larges variance in CMR_{GLC} included seven regions in the salience ventral attention network: the bilateral prefrontal cortex (29% and 20%), the bilateral frontal (29% and 26%) and parietal cortices (25% and 27%) and insula (25%). A relatively large proportion of variance in CMR_{GLC} was also explained in the left and right dorsal prefrontal cortex (23% to 30%) in the default mode network; the bilateral postcentral cortex (24% to 30%) and frontal eye field (34%) in the dorsal attention network; and the left and right lateral prefrontal cortex in the control network (25% and 28%).

The regions for which age explained the largest proportion of additional variance beyond cortical thickness included: the ventral prefrontal cortex (24% and 14%) and bilateral medial prefrontal cortex (19% and 18%) in the default mode network; the bilateral orbital frontal cortex in the limbic network (18% and 19%); the left post central cortex in the dorsal attention network (15%); and bilateral insula (17% and 12%), parietal operculum (11% and 14%), and right medial posterior prefrontal cortex (16%) in the salience ventral attention network. The regions for which age explained the lowest amount of additional variance included several visual regions (1% to 2%), the left post central region in the dorsal attention network (2%) and the right inferior parietal lobule (1%) in the default mode network.

3.4 Insulin Resistance, Cortical Thickness and CMR_{GLC} (Hypothesis 2)

HOMA-IR and Cortical Thickness

Although we did not find an association between HOMA-IR and cortical thickness in any region, we found an age group x HOMAIR interactions for cortical thickness in 40 of 100 regions (Figure 3 and table S3). In 32 of the 40 interactions identified, greater insulin resistance was associated with greater cortical thickness in younger adults but not in older adults (Figure 3c). In the remaining 8 regions, greater insulin resistance was associated with lower cortical thickness in older but not younger adults (Figure 3d). For older adults, a 10% increase in HOMA-IR was associated with 0% to 0.9% lower cortical thickness; and a mix of smaller positive and negative associations for younger adults ranging from -0.2% to +0.8% for each 10% increase in HOMA-IR (Table S3).

HOMA-IR and CMR_{GLC}

Higher insulin resistance was associated with lower CMR_{GLC} in the Schaefer 100 regions and subcortical structures after controlling for age (see Figure 4 and Table S4). Age explained

between 2% and 34% of the variance in CMR_{GLC} in the 100 regions. The regions for which age explained the largest amount of variance in CMR_{GLC} included: the bilateral dorsal and medial prefrontal cortices (30% to 34%) in the default mode network; the left insula (27% and 30%), the bilateral medial posterior prefrontal cortex and lateral prefrontal cortex in the salience ventral attention network (25% to 32%). Nine of the regions in the visual network were among the lowest in terms of the variance in CMR_{GLC} explained by age (2% to 9%).

HOMA-IR explained 4% to 12% of additional variance in CMR_{GLC} beyond age (block 2, the effect of HOMA-IR on CMR_{GLC}). These additional increases in variance were seen in regions across all networks, with the largest being in the bilateral precuneus (11% to 12%) and the right inferior parietal lobule (10%), posterior cingulate (10%) and lateral prefrontal cortex (9%) in the control network; and the right and left thalamus (10% and 9%). Three regions within the default network also showed some of the largest increases in variance from HOMA-IR: the left superior parietal lobule (12%) and the bilateral posterior cingulate cortex (both 10%). The left parietal medial cortex (9%) and bilateral parietal operculum (8% and 9%) within the salience/ventral attention network were also among the regions with the largest increases in variance explained by HOMA-IR. HOMA-IR explained the least amount of variance in a number of regions in the visual network and the bilateral putamen.

For the interaction of age and HOMA-IR, higher insulin resistance was associated with significantly lower CMR_{GLC} for younger adults, with a 10% increase in HOMA-IR associated with 4% to 8% lower CMR_{GLC} across regions; and smaller negative associations for older adults in the order of -1% to -3% for each 10% increase in CMR_{GLC} (see Figure 5 and Supplementary Table S4).

3.5 CMR_{GLC} and Cognition (Hypothesis 3)

Five principal components (PCs) of cognition with eigenvalues greater than one were identified across the six cognitive tests and eleven measures, explaining 80% of the variance. The varimax rotation also converged in five iterations (see Table S7). The first principal component loaded most strongly on cognitive control (task-switching and FSIQ). The second principal component loaded most strongly on response inhibition (stop-signal), the third component on episodic memory (verbal learning and digit substitution), the fourth component on working memory (digit

span) and fifth component on processing speed (reaction time on task-switching and digit substitution).

Higher CMR_{GLC} in the visual central and control networks was associated with better performance on the second principal component: response inhibition (Table 3). Higher CMR_{GLC} in the salience ventral attention, limbic, control and temporal parietal networks was associated with better performance on processing speed (principal component 5). Higher CMR_{GLC} in the subcortical region was also moderately associated with better performance on this principal component ($p = .078$). Higher CMR_{GLC} in the default network was associated with better performance on cognitive control.

None of the interaction terms of HOMA-IR and regional CMR_{GLC} were significant when added to the above multivariate models.

4. Discussion

4.1 The Association Between Older Age and Lower CMR_{GLC} is Partly Mediated by Cortical Atrophy

To our knowledge this is the first study to assess the relationship between age and cerebral rates of glucose metabolism at a spatial resolution of 100 brain regions while controlling for grey matter differences at the same scale. Our results support those from other studies that older age is associated with lower glucose metabolism and lower cortical thickness[2]. We add to this knowledge by highlighting that studies of age and cerebral metabolism need to account for age-related loss of brain volume as these reductions in brain tissue also led to reductions in measures of cerebral metabolism. We found that lower cerebral glucose metabolism in older versus younger adults is explained in part, but not in full, by cortical atrophy, with the mediating effect size varying by region. Cortical thickness explained between 0% and 34% of the variance in CMR_{GLC} in the 100 regions and subcortical structures, with age explaining 0% to 24% of additional variance depending on the region.

The results identified a positive relationship between higher cortical thickness and higher cerebral glucose metabolism in 83 of the 100 regions. The non-significant associations were primarily in the visual network. An age group x HOMA-IR interaction was also found in 40 regions for cortical thickness. A 10% increase in HOMA-IR was associated with a 0.1% to 0.8% lower cortical thickness in older adults. The older adults' mean cortical thickness was 240mm, hence these

associations correspond to approximately 0.24mm to 1.9mm decrease for every 10% increase in HOMA-IR, depending on the region. The effect for younger adults is smaller and more variable across the regions (see Figure 3 and Table S3).

The age group x HOMA-IR interaction for cortical thickness possibly relates to the difference in insulin levels among the age groups or their sensitivity to the actions of insulin; differences that may be differentially acting directly on cell growth and maintenance, rather than via glycaemic control assessed with HOMA-IR. In particular, although not statistically significant, our older adult group had a lower mean insulin level than the younger group. Insulin and insulin-like growth factor modulate brain cell growth and proliferation through downstream signalling of cell division, protein synthesis, and other anabolic pathways.[45] Hence, it is possible that insulin is contributing to growth or protection of grey matter as the brain develops and reaches its peak thickness in mid-life, after which lower insulin levels deleteriously impact insulin-related growth signalling, possibly through lower insulin production or greater resistance to the actions of insulin. This hypothesis is consistent with research showing a quadratic relationship between age and grey matter volume.[46,47] Our finding of lower cortical thickness among older adults is in line with previous research and has been well described. Age-related atrophy of grey matter is primarily due to neuronal shrinkage and reductions in synaptic density, including reductions in the length, number and distribution of dendritic spines on neurons.[48,49] Additional research is needed to directly assess whether or not insulin-related processes change across the adult lifespan in the brain and moderate cortical atrophy.

We found older age (controlling for cortical thickness) and higher insulin resistance to be associated with lower CMR_{GLC} in most brain regions. Lower correlations were seen in all 100 regions and subcortical structures for the partial correlation between age group and CMR_{GLC} controlling for cortical thickness versus the simple correlation between age and CMR_{GLC} (see Table S2 and Figure 2). However, in all cases the partial correlations remained above zero. These results suggest that cortical thickness mediates, in part but not in full, lower CMR_{GLC} among older adults.

The cerebral metabolism results in regions in the salience ventral attention network are noteworthy for several reasons. First, the salience ventral attention network is where cortical thickness explained the most variance in regional CMR_{GLC}, including in the left lateral prefrontal

cortex and insula and bilateral frontal and medial cortices. Second, the salience ventral attention network is also where age explained the most additional variance in regional CMR_{GLC} beyond cortical thickness differences, including in the left parietal medial cortex and insula, and the bilateral parietal operculum. A similar pattern was found among regions of the default network. Cortical thickness in the left and right dorsal prefrontal cortex explained a relatively high percentage of variance in CMR_{GLC}. Those same regions, together with the bilateral ventral and medial prefrontal cortices, showed some of the highest age-related additions in variance explained beyond cortical thickness. In contrast, CMR_{GLC} in regions of the limbic network was explained more by age than by grey matter differences. In particular, age explained twice the variance of cortical thickness in the left and right orbital frontal cortex and the right temporal pole. Taken together, the results suggest that regions of the salience ventral attention and default mode networks are most vulnerable to metabolic reductions from both atrophy and ageing, whereas the effect of age is stronger than the cortical thickness effect in regions of the limbic network. As noted, the regions in which age explained the largest proportion of additional variance in cortical thickness include the prefrontal and orbital frontal cortices and insula; the right temporal region within the control network; and the left and right temporal poles in the limbic network. These results are consistent with our recent meta-analyses showing that CMR_{GLC} differences in ageing are largest in the frontal and temporal regions and the insula.[2]

Cortical thickness explained more than 10% of the variance in CMR_{GLC} in five of eight subcortical structures. Adding age explained a relatively small amount of additional variance (2% to 7%). Of particular note was the small 3% and 2% of additional variance explained in CMR_{GLC} in the left and right caudate, respectively; the subcortical structure showing the largest CMR_{GLC} reductions in previous meta-analyses.[2] Our results suggest that age-related differences in CMR_{GLC} in the subcortical structures are strongly mediated by grey matter differences, and that it is especially important to take age-related atrophy into account when studying glucose metabolism in these structures.

The visual network also warrants highlighting because we could not explain significant variance in CMR_{GLC} with any of the independent variables. For example, cortical thickness accounted for a relatively small amounts of variance in CMR_{GLC}. Moreover, adding age and HOMA-IR explained relatively small amounts of additional variance in the stepwise regression models. These results

suggest that metabolism in the regions of the visual network is relatively robust to ageing and increased insulin resistance. Our results are consistent with studies indicating that the most prominent age-related reductions in cortical atrophy are in the fronto-temporal regions as opposed to the posterior regions.[49,50] Our findings suggest that the topology of age-related reductions in CMR_{GLC} follow a similar pattern.

4.2 The CMR_{GLC} and Insulin Resistance Relationship is Moderated by Age and is Independent of Grey Matter.

This is the first study to directly assess the relationship between insulin resistance and CMR_{GLC} among both younger and older adults free from a diagnosis of insulin resistance or Type 2 diabetes. In support of *hypothesis 2*, we found that higher insulin resistance was associated with lower CMR_{GLC} in most regions after controlling for age. The insulin resistance effect on cerebral glucose metabolism was independent of grey matter differences. As hypothesised, it was also moderated by age, indicated by the age group x HOMA-IR interaction. However, the negative effect of insulin resistance on CMR_{GLC} was stronger for younger than older adults in many brain regions, a finding inconsistent with our hypothesis. A 10% increase in HOMA-IR was associated with 4% to 8% lower CMR_{GLC} across regions for younger adults and 1% to 3% lower CMR_{GLC} for older adults. Based on the mean CMR_{GLC} across the regions and subcortical structures for each group, this corresponds to a reduction in glucose across regions of approximately 0.10 to 0.30 mg / 100ml / min for every 10% increase in HOMA-IR for younger adults, and .03 to .09 mg / 100ml / min for older adults. We also observed substantial variation in HOMA-IR in our sample, with values ranging from 0.6 to 3.25 in younger and 0.1 to 3.14 in older adults. Taken together, these results highlight that considerable differences in the rate of cerebral glucose metabolism can be expected from individual differences in insulin resistance, even in metabolically healthy adults.

Our results that higher insulin resistance is associated with lower CMR_{GLC} are consistent with a growing body of research suggesting that the brain is insulin sensitive and uses insulin in a wide range of functions.[51,52] The mechanism driving the insulin association with CMR_{GLC} in the brain remain to be fully elucidated. However, studies linking peripheral insulin function to brain changes include metabolic disturbances from an increase in neuronal insulin resistance, impaired insulin signalling, a pro-inflammatory state and mitochondrial dysfunction.[53] Prolonged peripheral

hyperinsulinemia can also decrease insulin receptors at the blood-brain barrier, thereby reducing insulin transport into the brain.[54] Much of the research in this area has been with participants with a diagnosis of insulin resistance or Type 2 diabetes[22] or been limited to older adults.[24,25,26] Our results suggest that further research assessing the insulin-dependent mechanisms affecting cerebral metabolism across a broader spectrum of insulin resistance levels and age ranges is warranted.

It is striking that the age group by HOMA-IR interaction indicated that higher insulin resistance was associated with greater CMR_{GLC} reductions in younger than older adults. This is somewhat counterintuitive, as we had expected that insulin resistance would be related to CMR_{GLC} reductions more so in older adults. While the reasons for these are not entirely clear, we note that our older adult sample had slightly lower mean and standard deviation fasting insulin and HOMA-IR levels than the younger adults (see Table 1; and Figure S1 in supplementary materials). This is in contrast to the association between ageing and increasing insulin resistance shown in several studies of the general population.[54,55] As such, our older cohort may be relatively insulin sensitive compared to the general older adult population. Replicating and extending our findings with other older adult populations with a wider range of insulin resistance levels is warranted.

4.3 CMR_{GLC} Primarily in "Higher Order" Brain Networks is Associated with Cognition

Our results partly support the hypothesis that cognitive function negatively correlates with CMR_{GLC} after controlling for cortical thickness and age, and the relationship is moderated by insulin resistance levels. We found associations between some measures of cognition and CMR_{GLC}, however, we did not find evidence of a moderating role of insulin resistance.

The regions associated with the largest age and insulin resistance-related CMR_{GLC} differences were primarily in the "higher order" networks (e.g., control and attention) as opposed to the primary processing networks (e.g., visual). This likely reflects the fact that the cognitive battery was designed to primarily index memory, spatiotemporal processing and attentional control. We also found higher CMR_{GLC}, primarily in the higher order networks, predicted performance on several factors from the PCA of cognitive tests. Improved processing speed (PC5) was associated with higher CMR_{GLC} in the salience ventral attention, limbic, control network and temporal parietal networks. Higher CMR_{GLC} in the default mode network and subcortex was associated with better cognitive control (PC1). A component measuring mostly response inhibition in the stop signal task

(i.e., reaction time) was negatively associated with CMR_{GLC} in the control and visual central networks, that is higher CMR_{GLC} was associated with faster reaction time.

We did not find significant CMR_{GLC} associations with episodic and working memory (PC3 and PC4). Unexpectedly, the age group effect for episodic and working memory were also not significant in the multivariate model with CMR_{GLC} and cortical thickness. A large body of research has shown that older adults typically show a decline in a number of cognitive domains compared with younger adults (for reviews see [56,57]). They include executive function, attention and memory.[57] These cognitive domains have been shown to peak in the third decade of life and then gradually decline.[58] Our results suggest that lower CMR_{GLC} in ageing may be driving some of the functional declines in attention, executive function and processing speed but not episodic and working memory. On the other hand, maintaining higher CMR_{GLC} in ageing may help retain better and faster task execution in attention, executive function and response inhibition. Additional research tracking longitudinal changes in CMR_{GLC} and cognition is recommended to test these proposed effects within individual over time, including whether memory changes are associated with alteration in CMR_{GLC}.

4.4 Implications for the Maintenance of Brain Health Across the Adult Lifespan

The results of the current study underscore the importance of insulin sensitivity to brain health across the adult lifespan – including at younger ages. Maintaining insulin sensitivity from early adulthood appears to be particularly important to ensuring optimal fuel for the brain, although it may also have a small and differential positive and negative effect on cortical thickness across regions. In contrast, from approximately the seventh decade onwards, maintaining insulin sensitivity my help to minimise age-related declines in cortical thickness, with a smaller benefit to CMR_{GLC} relative to younger adults. Diet, lifestyle (e.g., sleep, exercise, stress), and genetics are all risk factors for a increases in insulin resistance and would appear to be targets for public health interventions and clinical application to optimise both peripheral and central glucose metabolism.[59,60] Pharmaceutical treatments designed for diabetes by targeting peripheral glucose lowering and bodyweight reductions have recently shown efficacy in phase 1 clinical trials.[61] These pharmaceuticals may also support glucose metabolism in the brain, reducing or even negating the effects of age and insulin resistance related declines. Research directly assessing the impact of these pharmaceuticals on CMR_{GLC} is warranted.

4.5 Limitations

The current study used a cross-sectional design. Although informative about age-and insulin resistance-related differences, it is correlational in nature, limiting conclusions about the causal relationship between age, insulin resistance and CMR_{GLC}. Drawing conclusions about causal pathways requires longitudinal research and/or causal analyses. It is also possible that the differences we found between groups reflects underlying cohort differences rather than age-related changes. As noted above, our older adult population appears to be particularly healthy and relatively homogenous, at least in terms of insulin resistance.

Our study is also limited by the absence of middle age adults. Research on structural and functional brain networks have reported quadratic trajectories of age differences, with an inflection point somewhere in the third to fifth decade of life (see ref[62], for review). However, the lack of middle aged adults in our study precludes the identification and quantification of ageing trajectories across the full adult lifespan. Additional research is needed to elucidate these patterns.

HOMA-IR is considered a reliable clinical and research tool for the assessment of levels of insulin resistance.[17] Nevertheless, a limitation of HOMA-IR is that it represents a single snapshot of the complex glucose-insulin system.[63] Future research using dynamic measures (e.g., hyperinsulinemic-euglycemic clamp or 2-hour glucose tolerance tests) could improve our understanding of the complexity of insulin signalling and metabolism in the periphery and the brain in ageing and across the spectrum of health and metabolic-related diseases.

4.6 Conclusion

Age-related reductions in cerebral glucose metabolism are mediated in part by lower cortical thickness in ageing. Lower cerebral metabolism in most regions of the brain is associated with higher insulin resistance after controlling for age, and is not significantly impacted by cortical thickness. The strongest age and insulin resistance effects were identified in the salience ventral attention, control and default mode networks. Higher metabolic rates in these brain networks are associated with improved performance on tasks involving higher order cognitive functions, such as spatiotemporal processing, executive function and attention. Our findings underscore the criticality of insulin sensitivity to brain health across the adult lifespan and the importance of optimising the supply of glucose to the brain to sustain cognitive function in ageing.

Funding Information: Jamadar is supported by an Australian National Health and Medical Research Council (NHMRC) Fellowship (APP1174164).

Author Contributions: Deery and Jamadar conceptualised and designed the paper and analyses. Liang, Di Paolo, Voigt, Murray, Siddiqui and Deery contributed to the acquisition and pre-processing of the data. Deery and Liang contributed to the analyses. Deery, Jamadar, Egan and Moran contributed to the interpretation of data, and reviewed the manuscript for important intellectual content. All authors approved the version to be published.

Disclosure Statement: The authors declare no conflicts of interest.

References

1. Mergenthaler, P., Lindauer, U., Dienel, G. A., & Meisel, A. (2013). Sugar for the brain: the role of glucose in physiological and pathological brain function. Trends in Neurosciences, 36(10), 587–597. https://doi.org/10.1016/j.tins.2013.07.001

2. Deery, H. A., Di Paolo, R., Moran, C., Egan, G. F., & Jamadar, S. D. (2023a). Lower brain glucose metabolism in normal ageing is predominantly frontal and temporal: A systematic review and pooled effect size and activation likelihood estimates meta-analyses. Human Brain Mapping, 44(3), 1251–1277. https://doi.org/10.1002/hbm.26119

3. Peters, R., White, D., Cleeland, C., & Scholey, A. (2020). Fuel for Thought? A Systematic Review of Neuroimaging Studies into Glucose Enhancement of Cognitive Performance. Neuropsychology Review, 30(2), 234–250. https://doi.org/10.1007/s11065-020-09431-x

4. Chen, Z., & Zhong, C. (2013). Decoding Alzheimer's disease from perturbed cerebral glucose metabolism: Implications for diagnostic and therapeutic strategies. Progress in Neurobiology, 108, 21–43. https://doi.org/10.1016/j.pneurobio.2013.06.004

5. Sokoloff, L., Reivich, M., Kennedy, C., Des Rosiers, M. H., Patlak, C. S., Pettigrew, K. D., Sakurada, O., & Shinohara, M. (1977). The [14C]deoxyglucose method for the measurement of local cerebral glucose utilization: theory, procedure, and normal values in the conscious and anesthetized albino rat. Journal of Neurochemistry, 28(5), 897–916. https://doi.org/10.1111/j.1471-4159.1977.tb10649.

6. Carson, R. E. (2003). Tracer kinetic modeling in PET. In Valk P. E., Bailey D. L., Townsend D. W., & Maisey M. N. (Eds.), Positron Emission Tomography: Basic Science and Clinical Practice. Springer Science & Business Media.

7. Patlak, C. S., & Blasberg, R. G. (1985). Graphical evaluation of blood-to-brain transfer constants from multiple-time uptake data. Generalizations. Journal of Cerebral Blood Flow and Metabolism, 5(4), 584–590. https://doi.org/10.1038/jcbfm.1985.87.

8. Dimitrakopoulou-Strauss, A., Pan, L., & Sachpekidis, C. (2021). Kinetic modeling and parametric imaging with dynamic PET for oncological applications: general considerations, current clinical applications, and future perspectives. European Journal of Nuclear Medicine and Molecular Imaging, 48(1), 21–39. https://doi.org/10.1007/s00259-020-04843-6

9. Yang, J., Hu, C., Guo, N., Dutta, J., Vaina, L. M., Johnson, K. A., Sepulcre, J., Fakhri, G. E., & Li, Q. (2017). Partial volume correction for PET quantification and its impact on brain network in Alzheimer's disease. Scientific Reports, 7(1), 13035. https://doi.org/10.1038/s41598-017-13339-7

10. Meltzer, C. C., Kinahan, P. E., Greer, P. J., Nichols, T. E., Comtat, C., Cantwell, M. N., Lin, M. P., & Price, J. C. (1999). Comparative evaluation of MR-based partial-volume correction schemes for PET. Journal of Nuclear Medicine, 40(12), 2053–2065.

11. Tanna, N. K., Kohn, M. I., Horwich, D. N., Jolles, P. R., Zimmerman, R. A., Alves, W. M., & Alavi, A. (1991). Analysis of brain and cerebrospinal fluid volumes with MR imaging: impact on PET data correction for atrophy. Part II. Aging and Alzheimer dementia. Radiology, 178(1), 123–130. https://doi.org/10.1148/radiology.178.1.1984290

12. Schaefer, A., Kong, R., Gordon, E. M., Laumann, T. O., Zuo, X. N., Holmes, A. J., Eickhoff, S. B., & Yeo, B. T. T. (2018). Local-Global Parcellation of the Human Cerebral Cortex from Intrinsic Functional Connectivity MRI. Cerebral cortex (New York, N.Y. : 1991), 28(9), 3095–3114. https://doi.org/10.1093/cercor/bhx179

13. Tzourio-Mazoyer, N., Landeau, B., Papathanassiou, D., Crivello, F., Etard, O., Delcroix, N., Mazoyer, B., & Joliot, M. (2002). Automated anatomical labeling of activations in SPM using a macroscopic anatomical parcellation of the MNI MRI single-subject brain. NeuroImage, 15(1), 273–289. https://doi.org/10.1006/nimg.2001.0978

14. Wilcox G. (2005). Insulin and insulin resistance. The Clinical Biochemist Reviews, 26(2), 19–39.

15. Nystrom, F. H., & Quon, M. J. (1999). Insulin signalling: metabolic pathways and mechanisms for specificity. Cellular signalling, 11(8), 563–574. https://doi.org/10.1016/s0898-6568(99)00025-x

16. Frazier, H. N., Ghoweri, A. O., Anderson, K. L., Lin, R. L., Porter, N. M., & Thibault, O. (2019). Broadening the definition of brain insulin resistance in aging and Alzheimer's disease. Experimental Neurology, 313, 79–87. https://doi.org/10.1016/j.expneurol.2018.12.007

17. Lee, S. H., Park, S. Y., & Choi, C. S. (2022). Insulin Resistance: From Mechanisms to Therapeutic Strategies. Diabetes & metabolism journal, 46(1), 15–37. https://doi.org/10.4093/dmj.2021.0280

18. Gutch, M., Kumar, S., Razi, S. M., Gupta, K. K., & Gupta, A. (2015). Assessment of insulin sensitivity/resistance. Indian journal of endocrinology and metabolism, 19(1), 160–164. https://doi.org/10.4103/2230-8210.146874

19. Menke, A., Knowler, W.C., Cowie, C.C. (2018). Physical and Metabolic Characteristics of Persons With Diabetes and Prediabetes. Chapter 9 in Cowie C.C., Casagrande S.S. & Menke A. (Eds), Diabetes in America (3rd edition). National Institute of Diabetes and Digestive and Kidney Diseases. Bethesda, US.

20. Sacks, D. B., Arnold, M., Bakris, G. L., Bruns, D. E., Horvath, A. R., Lernmark, Å., Metzger, B. E., Nathan, D. M., & Kirkman, M. S. (2023). Guidelines and Recommendations for Laboratory Analysis in the Diagnosis and Management of Diabetes Mellitus. Clinical chemistry, hvad080. Advance online publication. https://doi.org/10.1093/clinchem/hvad080

21. Tomic, D., Shaw, J. E., & Magliano, D. J. (2022). The burden and risks of emerging complications of diabetes mellitus. Nature reviews. Endocrinology, 18(9), 525–539. https://doi.org/10.1038/s41574-022-00690-7

22. Macpherson, H., Formica, M., Harris, E., & Daly, R. M. (2017). Brain functional alterations in Type 2 Diabetes - A systematic review of fMRI studies. Frontiers in Neuroendocrinology, 47, 34–46. https://doi.org/10.1016/j.yfrne.2017.07.001

23. Chen, Y., Qiu, C., Yu, W., Shao, X., Zhou, M., Wang, Y., & Shao, X. (2022). The relationship between brain glucose metabolism and insulin resistance in subjects with normal cognition - a study based on 18F-FDG PET. Nuclear medicine communications, 43(3), 275–283. https://doi.org/10.1097/MNM.0000000000001511

24. Willette, A. A., Bendlin, B. B., Starks, E. J., Birdsill, A. C., Johnson, S. C., Christian, B. T., Okonkwo, O. C., La Rue, A., Hermann, B. P., Koscik, R. L., Jonaitis, E. M., Sager, M. A., & Asthana, S. (2015). Association of Insulin Resistance With Cerebral Glucose Uptake in Late Middle-Aged Adults at Risk for Alzheimer Disease. JAMA neurology, 72(9), 1013–1020. https://doi.org/10.1001/jamaneurol.2015.0613

25. Ishibashi, K., Onishi, A., Fujiwara, Y., Ishiwata, K., & Ishii, K. (2017). Effects of glucose, insulin, and insulin resistance on cerebral 18F-FDG distribution in cognitively normal older subjects. PloS one, 12(7), e0181400. https://doi.org/10.1371/journal.pone.0181400

26. Castellano, C. A., Hudon, C., Croteau, E., Fortier, M., St-Pierre, V., Vandenberghe, C., Nugent, S., Tremblay, S., Paquet, N., Lepage, M., Fülöp, T., Turcotte, É. E., Dionne, I. J., Potvin, O., Duchesne, S., & Cunnane, S. C. (2019). Links Between Metabolic and Structural Changes in the Brain of Cognitively Normal Older Adults: A 4-Year Longitudinal Follow-Up. Frontiers in aging neuroscience, 11, 15. https://doi.org/10.3389/fnagi.2019.00015

27. Hulman, A., Simmons, R. K., Brunner, E. J., Witte, D. R., Færch, K., Vistisen, D., Ikehara, S., Kivimaki, M., & Tabák, A. G. (2017). Trajectories of glycaemia, insulin sensitivity and insulin secretion in South Asian and white individuals before diagnosis of type 2 diabetes: a longitudinal analysis from the Whitehall II cohort study. Diabetologia, 60(7), 1252–1260. https://doi.org/10.1007/s00125-017-4275-6

28. Jamadar, S. D., Liang, E. X., Zhong, S., Ward, P. G. D., Carey, A., McIntyre, R., Chen, Z., & Egan, G. F. (2022). Monash DaCRA fPET-fMRI: A dataset for comparison of radiotracer administration for high temporal resolution functional FDG-PET. GigaScience, 11, giac031. https://doi.org/10.1093/gigascience/giac031

29. Dale, A. M., Fischl, B., & Sereno, M. I. (1999). Cortical surface-based analysis. I. Segmentation and surface reconstruction. NeuroImage, 9(2), 179–194. https://doi.org/10.1006/nimg.1998.0395

30. Fischl, B., & Dale, A. M. (2000). Measuring the thickness of the human cerebral cortex from magnetic resonance images. Proceedings of the National Academy of Sciences of the United States of America, 97(20), 11050–11055. https://doi.org/10.1073/pnas.200033797

31. Winkler, A. M., Kochunov, P., Blangero, J., Almasy, L., Zilles, K., Fox, P. T., Duggirala, R., & Glahn, D. C. (2010). Cortical thickness or grey matter volume? The importance of selecting the phenotype for imaging genetics studies. NeuroImage, 53(3), 1135–1146. https://doi.org/10.1016/j.neuroimage.2009.12.028

32. Burgos, N., Cardoso, M. J., Thielemans, K., Modat, M., Pedemonte, S., Dickson, J., Barnes, A., Ahmed, R., Mahoney, C. J., Schott, J. M., Duncan, J. S., Atkinson, D., Arridge, S. R., Hutton, B. F., & Ourselin, S. (2014). Attenuation correction synthesis for hybrid PET-MR scanners: application to brain studies. IEEE Transactions on Medical Imaging, 33(12), 2332–2341. https://doi.org/10.1109/TMI.2014.2340135.

33. Jenkinson, M., Bannister, P., Brady, M., & Smith, S. (2002). Improved optimization for the robust and accurate linear registration and motion correction of brain images. NeuroImage, 17(2), 825–841. https://doi.org/10.1016/s1053-8119(02)91132-8

34. Greve, D. N., Salat, D. H., Bowen, S. L., Izquierdo-Garcia, D., Schultz, A. P., Catana, C., Becker, J. A., Svarer, C., Knudsen, G. M., Sperling, R. A., & Johnson, K. A. (2016). Different partial volume correction methods lead to different conclusions: An (18)F-FDG-PET study of aging. NeuroImage, 132, 334–343. https://doi.org/10.1016/j.neuroimage.2016.02.042.

35. Greve, D. N., Svarer, C., Fisher, P. M., Feng, L., Hansen, A. E., Baare, W., Rosen, B., Fischl, B., & Knudsen, G. M. (2014). Cortical surface-based analysis reduces bias and variance in kinetic modeling of brain PET data. NeuroImage, 92, 225–236. https://doi.org/10.1016/j.neuroimage.2013.12.021

36. Graham, M. M., Muzi, M., Spence, A. M., O'Sullivan, F., Lewellen, T. K., Link, J. M., & Krohn, K. A. (2002). The FDG lumped constant in normal human brain. Journal of Nuclear Medicine, 43(9), 1157–1166.

37. Jamadar, S. D., Ward, P. G. D., Close, T. G., Fornito, A., Premaratne, M., O'Brien, K., Stäb, D., Chen, Z., Shah, N. J., & Egan, G. F. (2020). Simultaneous BOLD-fMRI and constant infusion FDG-PET data of the resting human brain. Scientific data, 7(1), 363. https://doi.org/10.1038/s41597-020-00699-5

38. Leenders, K. L., Perani, D., Lammertsma, A. A., Heather, J. D., Buckingham, P., Healy, M. J., Gibbs, J. M., Wise, R. J., Hatazawa, J., & Herold, S. (1990). Cerebral blood flow, blood volume and oxygen utilization. Normal values and effect of age. *Brain*, *113 (Pt 1)*, 27–47. https://doi.org/10.1093/brain/113.1.27

39. Matthews, D. R., Hosker, J. P., Rudenski, A. S., Naylor, B. A., Treacher, D. F., & Turner, R. C. (1985). Homeostasis model assessment: insulin resistance and beta-cell function from fasting plasma glucose and insulin concentrations in man. Diabetologia, 28(7), 412–419. https://doi.org/10.1007/BF00280883

40. Baron, R. M., & Kenny, D. A. (1986). The moderator-mediator variable distinction in social psychological research: conceptual, strategic, and statistical considerations. Journal of personality and social psychology, 51(6), 1173–1182. https://doi.org/10.1037//0022-3514.51.6.1173

41. Hayes, A. F. (Ed). (2017). Introduction to Mediation, Moderation, and Conditional Process Analysis: A Regression-Based Approach. Guilford Publications (2nd Edition). Hill, M. A., ISBN 9781462549030

42. Raghunathan, T. E., Rosenthal, R., & Rubin, D. B. (1996). Comparing correlated but nonoverlapping correlations. Psychological Methods, 1(2), 178–183. https://doi.org/10.1037/1082-989X.1.2.178

43. Benjamini, Y. & Hochberg, Y. (1995). Controlling the False Discovery Rate: A Practical and Powerful Approach to Multiple Testing. Journal of the Royal Statistical Society, Series B, 57, 289-300. https://doi.org/10.1111/j.2517-6161.1995.tb02031.x

44. Tabachnick, B.G. & Fidell L.S. (Eds.) (2018) Using Multivariate Statistics (7th Edition). Pearson, London, UK.

45. Milstein, J. L., & Ferris, H. A. (2021). The brain as an insulin-sensitive metabolic organ. Molecular metabolism, 52, 101234. https://doi.org/10.1016/j.molmet.2021.101234

46. Battaglini, M., Gentile, G., Luchetti, L., Giorgio, A., Vrenken, H., Barkhof, F., Cover, K. S., Bakshi, R., Chu, R., Sormani, M. P., Enzinger, C., Ropele, S., Ciccarelli, O., Wheeler-Kingshott, C., Yiannakas, M., Filippi, M., Rocca, M. A., Preziosa, P., Gallo, A., Bisecco, A., … MAGNIMS Study Group (2019). Lifespan normative data on rates of brain volume changes. Neurobiology of Aging, 81, 30–37. https://doi.org/10.1016/j.neurobiolaging.2019.05.010

47. Sigurdsson, S., Aspelund, T., Forsberg, L., Fredriksson, J., Kjartansson, O., Oskarsdottir, B., Jonsson, P. V., Eiriksdottir, G., Harris, T. B., Zijdenbos, A., van Buchem, M. A., Launer, L. J., & Gudnason, V. (2012). Brain tissue volumes in the general population of the elderly: the AGES-Reykjavik study. NeuroImage, 59(4), 3862–3870. https://doi.org/10.1016/j.neuroimage.2011.11.024

48. Pannese E. (2011). Morphological changes in nerve cells during normal aging. Brain structure & function, 216(2), 85–89. https://doi.org/10.1007/s00429-011-0308-y

49. Fjell, A. M., & Walhovd, K. B. (2010). Structural brain changes in aging: courses, causes and cognitive consequences. Reviews in the neurosciences, 21(3), 187–221. https://doi.org/10.1515/revneuro.2010.21.3.187

50. Fjell, A. M., McEvoy, L., Holland, D., Dale, A. M., Walhovd, K. B., & Alzheimer's Disease Neuroimaging Initiative (2014). What is normal in normal aging? Effects of aging, amyloid and

Alzheimer's disease on the cerebral cortex and the hippocampus. Progress in neurobiology, 117, 20–40. https://doi.org/10.1016/j.pneurobio.2014.02.004

51. Iozzo, P., & Guzzardi, M. A. (2019). Imaging of brain glucose uptake by PET in obesity and cognitive dysfunction: life-course perspective. Endocrine Connections, 8(11), R169–R183. https://doi.org/10.1530/EC-19-0348

52. Kullmann, S., Heni, M., Hallschmid, M., Fritsche, A., Preissl, H., & Häring, H. U. (2016). Brain Insulin Resistance at the Crossroads of Metabolic and Cognitive Disorders in Humans. Physiological Reviews, 96(4), 1169–1209. https://doi.org/10.1152/physrev.00032.2015

53. Bello-Chavolla, O. Y., Antonio-Villa, N. E., Vargas-Vázquez, A., Ávila-Funes, J. A., & Aguilar-Salinas, C. A. (2019). Pathophysiological Mechanisms Linking Type 2 Diabetes and Dementia: Review of Evidence from Clinical, Translational and Epidemiological Research. Current diabetes reviews, 15(6), 456–470. https://doi.org/10.2174/1573399815666190129155654

54. Elahi, D., Muller, D. C., McAloon-Dyke, M., Tobin, J. D., & Andres, R. (1993). The effect of age on insulin response and glucose utilization during four hyperglycemic plateaus. Experimental gerontology, 28(4-5), 393–409. https://doi.org/10.1016/0531-5565(93)90066-m

55. Paolisso, G., Scheen, A., & Lefèbvre, P. (1995). Glucose handling, diabetes and ageing. Hormone research, 43(1-3), 52–57. https://doi.org/10.1159/000184237

56. Brown, S. C., & Park, D. C. (2003). Theoretical models of cognitive aging and implications for translational research in medicine. The Gerontologist, 43 Spec No 1, 57–67. https://doi.org/10.1093/geront/43.suppl_1.57

57. Glisky, E. L. (2007). Changes in Cognitive Function in Human Aging. In D. R. Riddle (Ed.), *Brain Aging: Models, Methods, and Mechanisms*. CRC Press/Taylor & Francis.

58. Harada, C. N., Natelson Love, M. C., & Triebel, K. L. (2013). Normal cognitive aging. Clinics in geriatric medicine, 29(4), 737–752. https://doi.org/10.1016/j.cger.2013.07.002

59. Uusitupa, M., Khan, T. A., Viguiliouk, E., Kahleova, H., Rivellese, A. A., Hermansen, K., Pfeiffer, A., Thanopoulou, A., Salas-Salvadó, J., Schwab, U., & Sievenpiper, J. L. (2019). Prevention of Type 2 Diabetes by Lifestyle Changes: A Systematic Review and Meta-Analysis. Nutrients, 11(11), 2611. https://doi.org/10.3390/nu11112611

60. Akintola, A. A., & van Heemst, D. (2015). Insulin, aging, and the brain: mechanisms and implications. Frontiers in endocrinology, 6, 13. https://doi.org/10.3389/fendo.2015.00013

61. Rosenstock, J., Frias, J., Jastreboff, A. M., Du, Y., Lou, J., Gurbuz, S., Thomas, M. K., Hartman, M. L., Haupt, A., Milicevic, Z., & Coskun, T. (2023). Retatrutide, a GIP, GLP-1 and glucagon receptor agonist, for people with type 2 diabetes: a randomised, double-blind, placebo and active-controlled, parallel-group, phase 2 trial conducted in the USA. Lancet (London, England), S0140-6736(23)01053-X. Advance online publication. https://doi.org/10.1016/S0140-6736(23)01053-X

62. Deery, H. A., Di Paolo, R., Moran, C., Egan, G. F., & Jamadar, S. D. (2023b). The older adult brain is less modular, more integrated, and less efficient at rest: A systematic review of large-scale resting-state functional brain networks in aging. Psychophysiology, 60(1), e14159. https://doi.org/10.1111/psyp.14159

63. Park, S. Y., Gautier, J. F., & Chon, S. (2021). Assessment of Insulin Secretion and Insulin Resistance in Human. Diabetes & metabolism journal, 45(5), 641–654. https://doi.org/10.4093/dmj.2021.0220

Figures

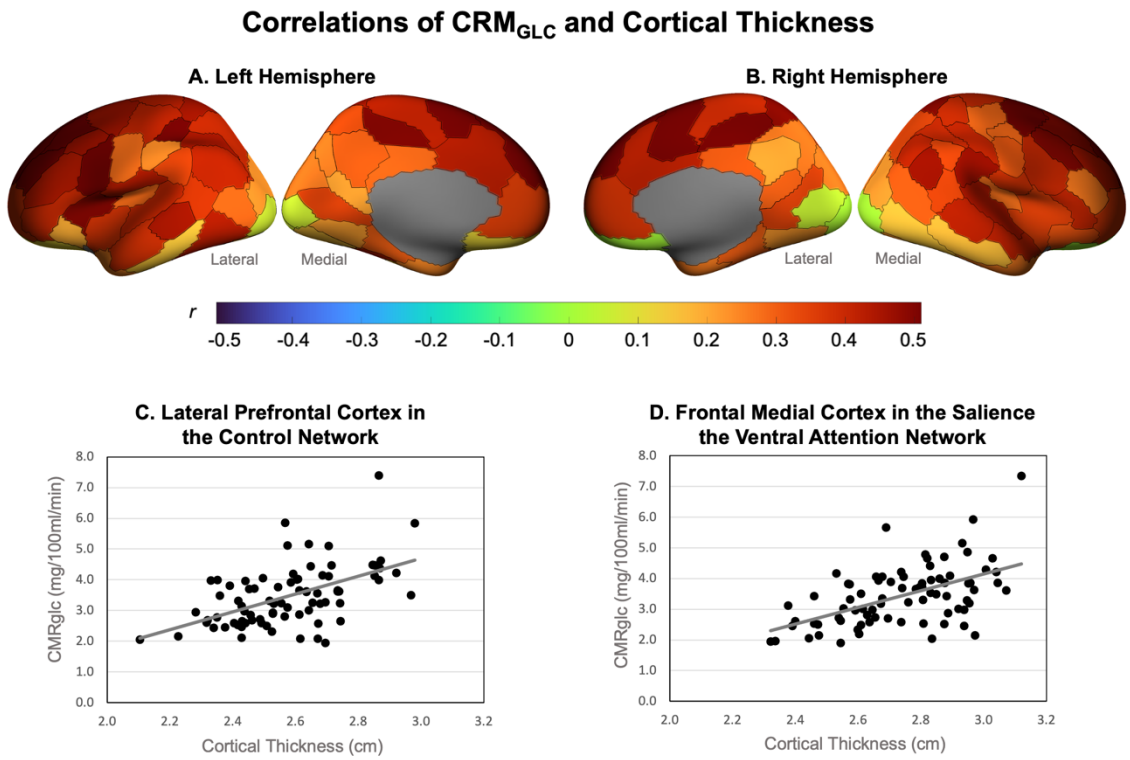

Figure 1. Correlation of CMR_{GLC} and cortical thickness in the Schaefer 100 regions in the (A) left and (B) right hemispheres (also see Table S2). Example correlations in (C) the lateral prefrontal cortex in the control network, and (D) the frontal medial cortex in the salience ventral attention network. Figures were produced using the toolbox at: https://github.com/StuartJO/plotSurfaceROIBoundary

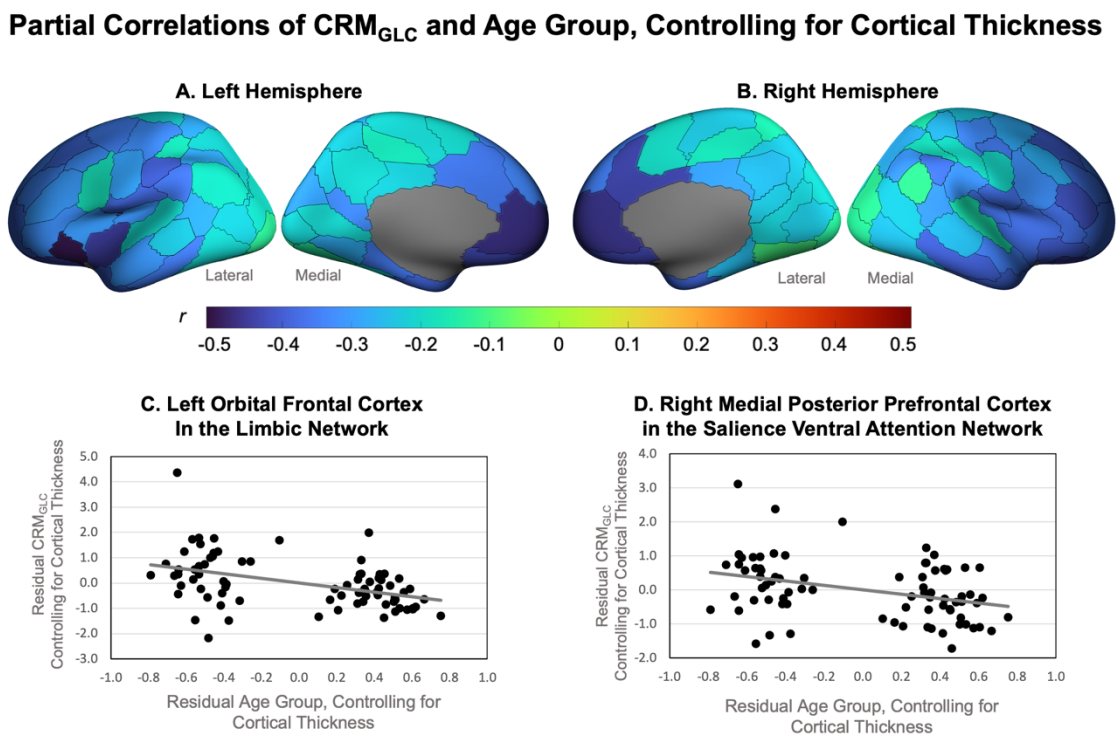

Figure 2. Partial correlation of CMR_{GLC} and age group, after controlling for cortical thickness in the Schaefer 100 regions in the (A) left and (B) right hemispheres. Example age group and CMR_{GLC} relationships in (C) the left orbital frontal cortex in the limbic network, and (D) the right medial posterior prefrontal cortex in the salience ventral attention network (younger group is on the left; older group on the right). The impact of potential outliers seen in (C) and (D) on the partial correlations was assessed via separate analyses excluding the outlier participants and log transforming the CMR_{GLC}, distribution to reduce non-normality caused by the outliers. The results were similar in all cases, with the largest difference in r of .03 across the analysis methods for each region (see supplementary materials, Figure S1).

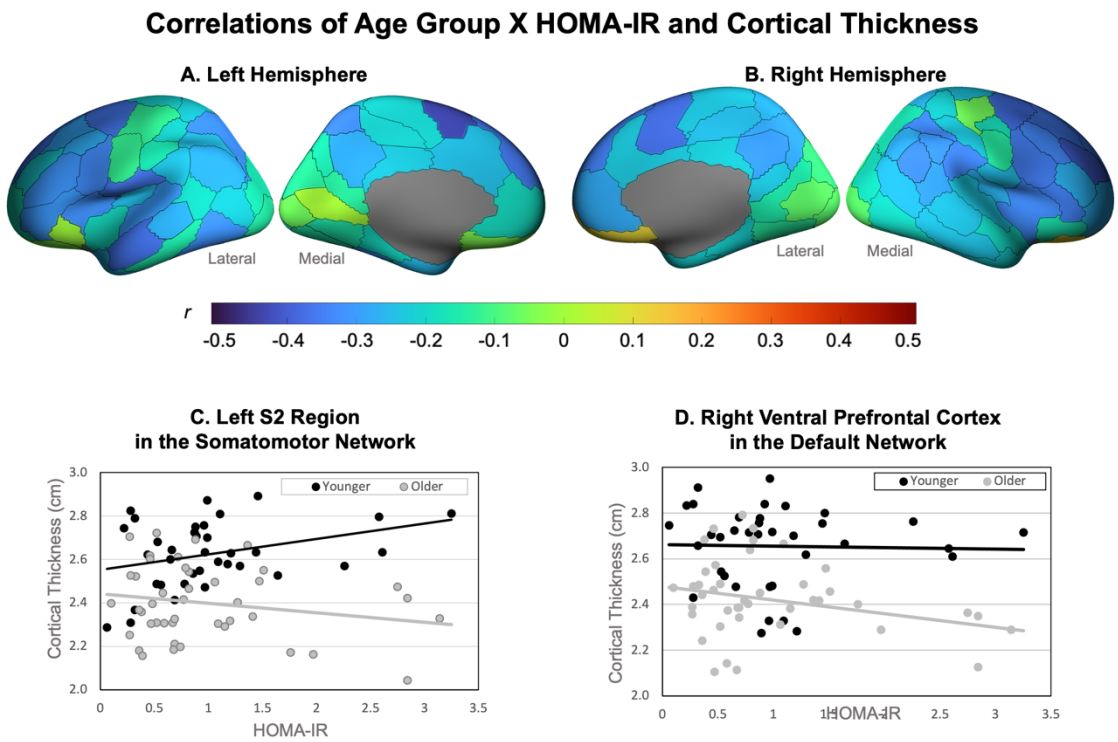

Figure 3. Age group X HOMA-IR interaction and cortical thickness correlations in Schaefer 100 regions in the (A) left and (B) right hemispheres. Example age group X HOMA-IR interactions in (C) left S2 region of the somatomotor network, (D) right ventral prefrontal cortex in the default network. Forty of the 100 regions show significant interactions (Table S3). (C) is representative of 32 (80%) of the brain regions where the correlation is positive for younger adults and negative for older adults; (D) is representative of eight (20%) of the interactions in which there is no correlation for younger adults but a negative correlation for older adults.

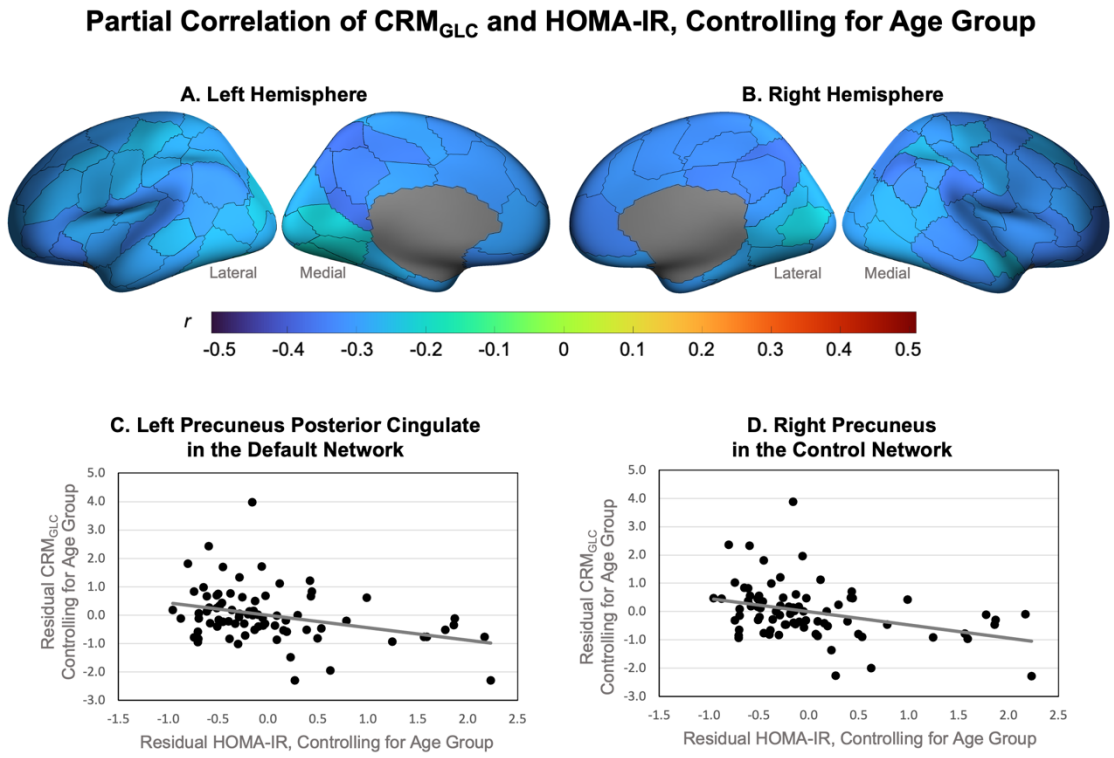

Figure 4. Partial correlation of CMR_{GLC} and HOMA-IR, controlling for age group in Schaefer 100 regions in (A) left and (B) right hemispheres. Example partial correlations in (C) the left precuneus posterior cingulate in the default network and, (D) right precuneus In the control network The impact of potential outliers seen in (C) and (D) on the partial correlations was assessed via separate analyses excluding the outlier participants and log transforming the CMR_{GLC}, distribution to reduce non-normality from the outliers. The results were similar in all brain regions, with the largest correlation coefficient difference being .03 across the analysis methods (see supplementary materials,

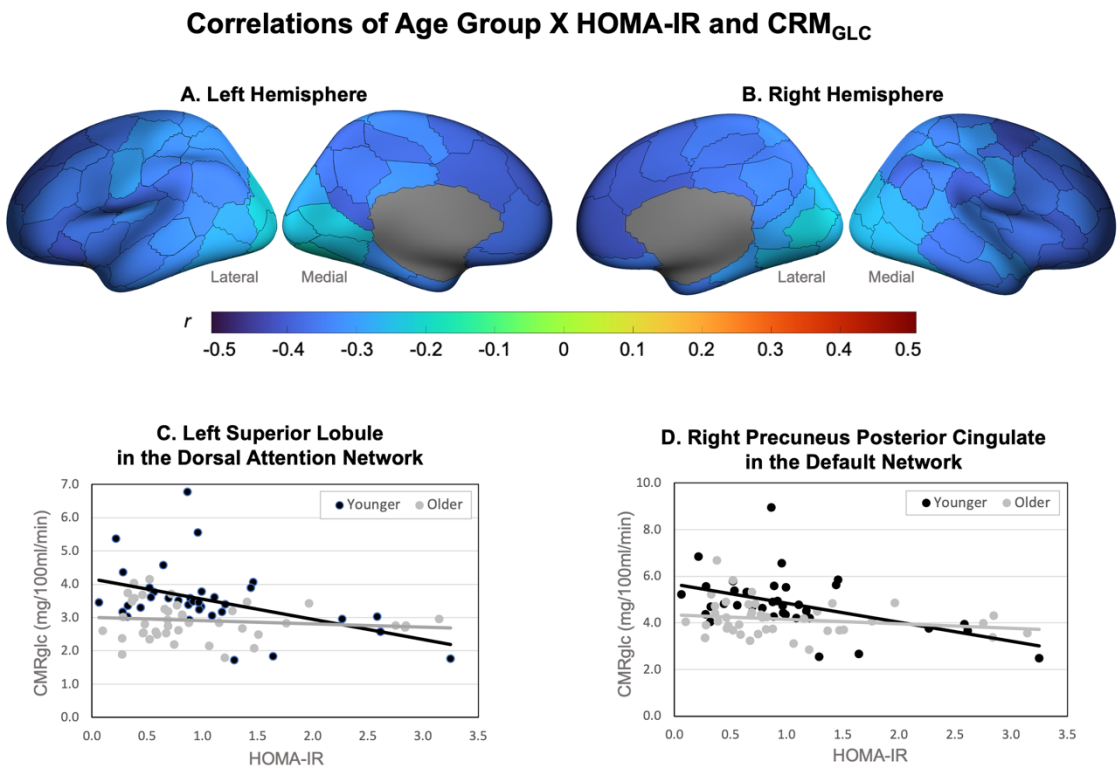

Figure 5. Correlations of age group X HOMA-IR interaction with CMR_{GLC} in Schaefer 100 regions in the (A) left and (B) right hemispheres. Example interactions in (C) the left superior lobule in the dorsal attention, and (D) right precuneus posterior cingulate in the default network.

Tables

Table 1. Demographics comparison of older and younger groups. Continuous variables are mean (standard deviation); categorical variables are %.

	Younger (N = 36)	Older (N = 43)	p-value[1]
Age (years)	27.8 (6.2)	75.5 (5.8)	<.001
Sex (% female)	58%	47%	0.295
Education (years)	18 (2.8)	16.9 (3.6)	0.167
Fasting blood glucose (mmol/L)	4.7 (0.3)	5.1 (0.5)	<.001
Fasting insulin (mIU/L)	4.7 (3.1)	4.0 (2.7)	0.268
HOMA_IR	1.0 (0.7)	0.9 (0.7)	0.783
Grey Matter Volume (mm^3)	487,646 (47,479)	425,474 (44,248)	<.001
Cortical Thickness (cm)	2.52 (0.07)	2.36 (0.11)	<.001
Systolic Blood Pressure	119.5 (17.6)	148.7 (24.3)	<.001
Diastolic Blood Pressure	79.4 (13.4)	83.6 (11.9)	0.144
Resting Heart Rate	82.6 (17.3)	73.9 (13)	0.013
BMI	24.1 (4.6)	25.6 (3.5)	0.133
Smoking (per 6 weeks)			
Never	85%	100%	0.127
On 1 day	3%	0%	
1-2 days in 6 weeks	6%	0%	
1-2 days in a week	0%	0%	
Everyday	6%	0%	
Alcohol (per 6 weeks)			
Never	29%	22%	0.033
On 1 day	12%	14%	
1-2 days in 6 weeks	29%	17%	
1-2 days in a week	29%	22%	
Everyday	0%	25%	
Recreational drugs (per 6 weeks)			
Never	97%	100%	0.300
On 1 day	0%	0%	
1-2 days in 6 weeks	0%	0%	
1-2 days in a week	3%	0%	
Everyday	0%	0%	

[1]P-values are based on T-test for continuous and Ch-square for categorical variables.

Table 2. Summary of primary analyses undertaken to test *hypotheses 1* and *2*. *Yes* indicates significant effect (p < .05, FDR-corrected; details of the analyses are in the supplementary materials, Tables S2 to S6).

Left Hemisphere								
	Hypothesis 1	Hypothesis 2						
	Is higher cortical thickness assocaited with higher CMRGLC?	Is older age associated with lower CMRGLC?	Is older age associated with lower CMRGLC, controlling for cortical thickness?	How much variance in CMRGLC is explained by cortical thickness and additional variance by age group		Is higher insulin resistance (HOMA-IR) associated with lower CMRGLC, controlling for age group?	% change in CMRGLC from 10% increase in HOMA-IR	
				Thickness	Age		Younger	Older
Visual Central: Extra Striate Cortex 1	No	No	No	3%	2%	Yes	-5%	-1%
Visual Central: Extra Striate Cortex 2	No	No	No	0%	2%	Yes	-7%	-1%
Visual Central: Striate Cortex 1	No	No	No	0%	5%	Yes	-7%	-1%
Visual Central: Extra Striate Cortex 3	No	Yes	No	5%	4%	Yes	-6%	0%
Visual Peripheral: Extra Striate Inferior 1	No	Yes	Yes	4%	7%	Yes	-5%	0%
Visual Peripheral: Striate Cortex Calcarine 1	Yes	Yes	No	12%	4%	Yes	-6%	0%
Visual Peripheral: Extra Striate CortexSup 1	Yes	Yes	Yes	7%	8%	Yes	-7%	0%
Somatomotor A: 1	Yes	Yes	Yes	17%	9%	Yes	-5%	0%
Somatomotor A: 2	Yes	Yes	No	18%	4%	Yes	-5%	-1%
Somatomotor B: Auditory 1	Yes	Yes	No	16%	3%	Yes	-6%	-1%
Somatomotor B: S2 1	Yes	Yes	Yes	8%	9%	Yes	-6%	-1%
Somatomotor B: S2 2	Yes	Yes	Yes	19%	12%	Yes	-6%	-1%
Somatomotor B: Central 1	Yes	Yes	Yes	8%	8%	Yes	-5%	-1%
Dorsal Attention A: Temporal Occipital 1	Yes	Yes	No	18%	3%	Yes	-5%	0%
Dorsal Attention A: Parietal Occipital 1	Yes	Yes	No	8%	5%	No	-5%	-1%
Dorsal Attention A: Superior Parietal Lobule 1	Yes	Yes	No	16%	4%	Yes	-6%	-1%
Dorsal Attention B: Post Central 1	Yes	Yes	Yes	6%	15%	Yes	-5%	-1%
Dorsal Attention B: Post Central 2	Yes	Yes	No	30%	2%	No	-5%	-1%
Dorsal Attention B: Post Central 3	Yes	Yes	Yes	20%	6%	Yes	-5%	-1%
Dorsal Attention B: Frontal Eye Fields 1	Yes	Yes	Yes	20%	9%	Yes	-5%	-1%
Salience Ventral Attention A: Parietal Operculum 1	Yes	Yes	Yes	12%	11%	Yes	-6%	-1%
Salience Ventral Attention A: Insula: 1	Yes	Yes	Yes	14%	17%	Yes	-5%	-1%
Salience Ventral Attention A: Insula: 2	Yes	Yes	Yes	25%	7%	Yes	-6%	-1%
Salience Ventral Attention A: Parietal Medial 1	Yes	Yes	No	25%	2%	Yes	-6%	-2%
Salience Ventral Attention A: Frontal Medial 1	Yes	Yes	No	27%	3%	No	-6%	-2%
Salience Ventral Attention B: Lateral Prefrontal Cortex 1	Yes	Yes	Yes	29%	8%	Yes	-6%	-2%
Salience Ventral Attention B: Medial Posterior Prefrontal 1	Yes	Yes	Yes	18%	10%	Yes	-5%	-2%
LimbiC: B: Orbital Frontal Cortex 1	No	Yes	Yes	1%	18%	No	-7%	-2%
LimbiC: A: Temporal Pole 1	Yes	Yes	Yes	6%	14%	Yes	-4%	-1%
LimbiC: A: Temporal Pole 2	No	Yes	Yes	2%	12%	Yes	-6%	-1%
Control A: Intraparietal Sulcus 1	Yes	Yes	Yes	20%	6%	Yes	-6%	-1%
Control A: Lateral Prefrontal Cortex 1	Yes	Yes	Yes	19%	7%	Yes	-6%	-1%
Control A: Lateral Prefrontal Cortex 2	Yes	Yes	No	28%	2%	No	-5%	-2%
Control B: Lateral Prefrontal Cortex 1	Yes	Yes	Yes	14%	12%	Yes	-7%	-1%
Control C: Precuneus 1	Yes	Yes	No	6%	5%	Yes	-8%	-3%
Control C: Precuneus 2	Yes	Yes	No	11%	4%	Yes	-7%	-2%
Control C: Cingulate Posterior 1	Yes	Yes	No	8%	5%	Yes	-6%	-1%
Default A: Dorsal Prefrontal Cortex 1	Yes	Yes	Yes	30%	10%	Yes	-6%	-2%
Default A: Precuneus Posterior Cingulate Cortex1	Yes	Yes	No	9%	4%	Yes	-7%	-3%
Default A: Medial Prefrontal Cortex 1	Yes	Yes	Yes	13%	19%	Yes	-5%	-1%
Default B: Temp 1	Yes	Yes	Yes	15%	8%	Yes	-5%	-1%
Default B: Temp 2	Yes	Yes	No	20%	4%	Yes	-5%	-1%
Default B: inferior parietal lobule 1	Yes	Yes	No	17%	3%	Yes	-6%	-1%
Default B: Dorsal Prefrontal Cortex 1	Yes	Yes	Yes	29%	8%	Yes	-6%	-2%
Default B: Lateral Prefrontal Cortex 1	Yes	Yes	Yes	21%	8%	Yes	-5%	-1%
Default B: Ventral Prefrontal Cortex 1	No	Yes	Yes	4%	24%	Yes	-6%	-2%
Default B: Ventral Prefrontal Cortex 2	Yes	Yes	Yes	16%	8%	Yes	-7%	-2%
Default C: RetroSuperior Parietal Lobuleenial 1	No	Yes	Yes	4%	10%	Yes	-8%	-3%
Default C: Parahippocampal Cortex 1	Yes	Yes	Yes	9%	11%	Yes	-4%	-1%
Temporal Parietal 1	Yes	Yes	Yes	14%	7%	Yes	-6%	-1%
Caudate		Yes	No	12%	3%	Yes	-3%	-1%
Putamen		Yes	Yes	12%	6%	Yes	-2%	-1%
Pallidum		Yes	Yes	11%	7%	Yes	-4%	0%
Thalamus		Yes	No	9%	4%	Yes	-5%	-1%

Right Hemisphere								
	Hypothesis 1	Hypothesis 2						
	Is higher cortical thickness assocaited with higher CMRGLC?	Is older age associated with lower CMRGLC?	Is older age associated with lower CMRGLC, controlling for cortical thickness?	How much variance in CMRGLC is explained by cortical thickness and additional variance by age group		Is higher insulin resistance (HOMA-IR) associated with lower CMRGLC, controlling for age group?	% change in CMRGLC from 10% increase in HOMA-IR	
				Thickness	Age		Younger	Older
Visual Central: Extra Striate Cortex 1	No	No	No	5%	1%	Yes	-6%	-1%
Visual Central: Extra Striate Cortex 2	No	No	No	0%	2%	Yes	-7%	0%
Visual Central: Extra Striate Cortex 3	No	No	No	5%	2%	Yes	-6%	-1%
Visual Peripheral: Striate Cortex Calcarine 1	No	Yes	No	0%	5%	No	-7%	-1%
Visual Peripheral: Extra Striate Inferior 1	Yes	Yes	No	12%	4%	Yes	-6%	-1%
Visual Peripheral: Extra Striate Superior 1	Yes	Yes	No	6%	4%	Yes	-6%	-1%
Somatomotor A: 1	Yes	Yes	Yes	8%	11%	Yes	-7%	-1%
Somatomotor A: 2	Yes	Yes	Yes	8%	10%	Yes	-5%	-1%
Somatomotor A: 3	Yes	Yes	Yes	15%	6%	Yes	-5%	-1%
Somatomotor A: 4	Yes	Yes	No	16%	5%	Yes	-5%	-1%
Somatomotor B: Auditory 1	Yes	Yes	No	20%	2%	Yes	-6%	0%
Somatomotor B: S2 1	Yes	Yes	Yes	7%	12%	Yes	-7%	0%
Somatomotor B: S2 2	Yes	Yes	Yes	14%	11%	Yes	-7%	-1%
Somatomotor B: Central 1	Yes	Yes	No	9%	3%	Yes	-5%	-1%
Dorsal Attention A: Temporal Occipital 1	No	Yes	No	2%	6%	Yes	-6%	-1%
Dorsal Attention A: Parietal Occipital 1	Yes	Yes	No	9%	5%	Yes	-5%	-2%
Dorsal Attention A: Superior Parietal Lobule 1	Yes	Yes	Yes	11%	6%	Yes	-5%	-1%
Dorsal Attention B: Post Central 1	Yes	Yes	No	16%	3%	Yes	-6%	-1%
Dorsal Attention B: Post Central 2	Yes	Yes	No	24%	2%	Yes	-5%	-2%
Dorsal Attention B: Frontal Eye Fields 1	Yes	Yes	Yes	34%	5%	Yes	-5%	-2%
Salience Ventral Attention A: Parietal Operculum 1	Yes	Yes	Yes	11%	14%	Yes	-6%	-1%
Salience Ventral Attention A: InsulA: 1	Yes	Yes	Yes	12%	12%	Yes	-6%	-2%
Salience Ventral Attention A: Parietal Medial 1	Yes	Yes	No	27%	2%	Yes	-5%	-2%
Salience Ventral Attention A: Frontal Medial 1	Yes	Yes	No	28%	3%	Yes	-6%	-2%
Salience Ventral Attention B: Inferior Parietal Lobule 1	Yes	Yes	Yes	11%	11%	Yes	-5%	-1%
Salience Ventral Attention B: Lateral Prefrontal Cortex 1	Yes	Yes	Yes	20%	10%	Yes	-6%	-1%
Salience Ventral Attention B: Medial Posterior Prefrontal 1	Yes	Yes	Yes	18%	16%	Yes	-6%	-1%
Limbic B: Orbital Frontal Cortex 1	No	Yes	Yes	0%	19%	Yes	-7%	-2%
Limbic A: Temporal Pole 1	Yes	Yes	Yes	7%	13%	Yes	-5%	-1%
Control A: Intraparietal Sulcus 1	Yes	Yes	No	16%	3%	Yes	-6%	-2%
Control A: Lateral Prefrontal Cortex 1	Yes	Yes	Yes	7%	16%	Yes	-7%	-2%
Control A: Lateral Prefrontal Cortex 2	Yes	Yes	Yes	16%	9%	Yes	-7%	-2%
Control B: Temporal 1	No	Yes	Yes	3%	15%	Yes	-6%	-2%
Control B: inferior parietal lobule 1	Yes	Yes	Yes	17%	8%	Yes	-7%	-2%
Control B: Lateral Prefrontal Cortexd 1	Yes	Yes	Yes	25%	5%	Yes	-8%	-2%
Control B: Lateral Prefrontal Cortexv 1	Yes	Yes	Yes	13%	11%	Yes	-6%	-2%
Control C Cingulate Posterior 1	Yes	Yes	Yes	9%	8%	Yes	-7%	-2%
Control C Precuneus 1	Yes	Yes	No	7%	5%	Yes	-7%	-2%
Default A: Inferior Parietal Lobule 1	Yes	Yes	No	21%	1%	Yes	-5%	-2%
Default A: Dorsal Prefrontal Cortex 1	Yes	Yes	Yes	23%	12%	Yes	-7%	-2%
Default A: Precuneus Posterior Cingulate Cortex 1	No	Yes	Yes	4%	6%	Yes	-7%	-2%
Default A: Medial Prefrontal Cortex 1	Yes	Yes	Yes	14%	18%	Yes	-6%	-1%
Default B: Dorsal Prefrontal Cortex 1	Yes	Yes	Yes	28%	9%	Yes	-7%	-1%
Default B: Ventral Prefrontal Cortex 1	Yes	Yes	Yes	10%	14%	Yes	-7%	0%
Default B: Ventral Prefrontal Cortex 2	Yes	Yes	Yes	16%	11%	Yes	-8%	-2%
Default C retroSuperior Parietal Lobuleenial 1	Yes	Yes	No	9%	5%	Yes	-7%	-1%
Default C Parahippocampal Cortex 1	Yes	Yes	Yes	9%	6%	Yes	-4%	-1%
Temporal Parietal 1	Yes	Yes	Yes	17%	10%	Yes	-3%	-1%
Temporal Parietal 2	Yes	Yes	Yes	18%	5%	Yes	-4%	-1%
Temporal Parietal 3	Yes	Yes	Yes	12%	5%	Yes	-4%	-1%
Caudate		Yes	No	9%	2%	Yes	-2%	-1%
Putamen		Yes	No	11%	5%	Yes	-2%	-1%
Pallidum		Yes	Yes	11%	6%	Yes	-3%	-2%
Thalamus		Yes	No	8%	3%	Yes	-5%	-3%

Table 3. Multivariate General Linear Model predicting 5 principal components of cognition from CMR_{GLC} in the Schaefer 17 Networks, age group and cortical thickness. Post-hoc tests for significant multivariate models are shown at $p < 0.10$.

	Multivariate General Linear Model (MANOVA)		Post-Hoc Test									
			Component 1		Component 2		Component 3		Component 4		Component 5	
Schaefer 17 Network	F	p	F	p	F	p	F	p	F	p	F	p
Visual Central	2.4	0.046	0.2	0.622	7.087	0.010	0.9	0.335	1.342	0.25	0.0	0.926
Visual Peripheral	1.1	0.382										
Somatomotor A	0.9	0.501										
Somatomotor B	0.5	0.809										
Dorsal Attention A	1.2	0.322										
Dorsal Attention B	1.6	0.172										
Salience Ventral Attention A	3.0	0.019	0.7	0.401	1.7	0.191	0.2	0.662	1.1	0.294	12.2	0.001
Salience Ventral Attention B	1.0	0.425										
Limbic A	0.5	0.788										
Limbic B	2.1	0.084	3.2	0.081	0.0	0.985	0.2	0.627	0.1	0.812	4.0	0.049
Control A	2.5	0.045	0.1	0.725	4.7	0.035	0.6	0.425	0.6	0.448	6.0	0.018
Control B	1.8	0.130										
Control C	1.6	0.175										
Default A	0.6	0.728										
Default B	0.9	0.466										
Default C	2.4	0.046	6.7	0.012	0.5	0.477	0.4	0.548	0.4	0.509	0.9	0.348
Temporal Parietal	2.3	0.055	1.9	0.176	2.2	0.142	1.8	0.189	1.3	0.261	4.2	0.046
Subcortical	2.0	0.096	4.9	0.031	1.2	0.288	0.4	0.521	0.0	0.841	3.2	0.078
Age Category	6.0	0.000	14.2	0.000	0.0	0.875	0.0	0.918	0.4	0.527	8.6	0.005
Cortical Thickness	0.9	0.458										